

Cell adhesion molecules regulate Ca^{2+} -mediated steering of growth cones via cyclic AMP and ryanodine receptor type 3

Noriko Ooashi,¹ Akira Futatsugi,² Fumie Yoshihara,¹ Katsuhiko Mikoshiba,² and Hiroyuki Kamiguchi¹

¹Laboratory for Neuronal Growth Mechanisms, Brain Science Institute, The Institute of Physical and Chemical Research, Saitama 351-0198, Japan

²Calcium Oscillation Project, International Cooperative Research Project, Japan Science and Technology Cooperation, Tokyo 108-0071, Japan

Axonal growth cones migrate along the correct paths during development, not only directed by guidance cues but also contacted by local environment via cell adhesion molecules (CAMs). Asymmetric Ca^{2+} elevations in the growth cone cytosol induce both attractive and repulsive turning in response to the guidance cues (Zheng, J.Q. 2000. *Nature*. 403:89–93; Henley, J.R., K.H. Huang, D. Wang, and M.M. Poo. 2004. *Neuron*. 44:909–916). Here, we show that CAMs regulate the activity of ryanodine receptor type 3 (RyR3) via cAMP and protein kinase A in dorsal root ganglion

neurons. The activated RyR3 mediates Ca^{2+} -induced Ca^{2+} release (CICR) into the cytosol, leading to attractive turning of the growth cone. In contrast, the growth cone exhibits repulsion when Ca^{2+} signals are not accompanied by RyR3-mediated CICR. We also propose that the source of Ca^{2+} influx, rather than its amplitude or the baseline Ca^{2+} level, is the primary determinant of the turning direction. In this way, axon-guiding and CAM-derived signals are integrated by RyR3, which serves as a key regulator of growth cone navigation.

Introduction

During neuronal development and regeneration, the growth cone navigates the axon toward its target by monitoring environmental cues along its path. Such environmental cues can be diffusible, substrate-bound or cell surface molecules, which serve as either attractants or repellents upon binding to relevant receptors expressed on the growth cone surface (Tessier-Lavigne and Goodman, 1996; Huber et al., 2003). Many guidance molecules, including netrin-1, NGF, brain-derived neurotrophic factor, and myelin-associated glycoprotein (MAG), influence the direction of axon extension through cytosolic Ca^{2+} signals in the growth cone (Song and Poo, 1999; Hong et al., 2000). It has also been shown that a focal and unilateral elevation of cytosolic free Ca^{2+} concentration ($[\text{Ca}^{2+}]_c$) in the growth cone is sufficient to induce its turning to the side with elevated $[\text{Ca}^{2+}]_c$ (Zheng, 2000). Interestingly, extracellular gradients of netrin-1 or MAG, which normally induce attractive or repulsive growth

cone turning, respectively, increase $[\text{Ca}^{2+}]_c$ that is highest on the side of the growth cone facing the source of the netrin-1/MAG gradients (Hong et al., 2000; Henley et al., 2004). This observation indicates that a $[\text{Ca}^{2+}]_c$ gradient across the growth cone can trigger turning to the side with higher $[\text{Ca}^{2+}]_c$ (attraction) as well as to the side with lower $[\text{Ca}^{2+}]_c$ (repulsion). What, then, determines the growth cone responses to the $[\text{Ca}^{2+}]_c$ gradient? An important distinction might be the amplitude of Ca^{2+} signals, with high-amplitude signals mediating attraction and low-amplitude signals mediating repulsion (Nishiyama et al., 2003; Henley et al., 2004; Wen et al., 2004). An earlier study showed that baseline $[\text{Ca}^{2+}]_c$ is a determinant of the growth cone responses to $[\text{Ca}^{2+}]_c$ increases: normal baseline $[\text{Ca}^{2+}]_c$ (~130 nM) favors attraction, and low baseline $[\text{Ca}^{2+}]_c$ (~60 nM) favors repulsion (Zheng, 2000). However, because cytosolic Ca^{2+} signals above some threshold level activate the ryanodine receptors (RyRs) on the internal Ca^{2+} stores (for review see Bouchard et al., 2003), high-level Ca^{2+} signals are likely to trigger secondary Ca^{2+} influx to the cytosol via RyRs, a process called Ca^{2+} -induced Ca^{2+} release (CICR). Therefore, it is possible that the differential turning responses of the growth cone to Ca^{2+} signals depend primarily on the source of Ca^{2+} influx rather than the amplitude or the baseline level of Ca^{2+} signals. Answering this question is an important

Correspondence to Hiroyuki Kamiguchi: kamiguchi@brain.riken.jp

Abbreviations used in this paper: AM, acetoxymethyl ester; BAPTA, 1,2-bis(o-aminophenoxy)ethane-N,N,N',N'-tetraacetic acid; $[\text{Ca}^{2+}]_c$, cytosolic free Ca^{2+} concentration; CAM, cell adhesion molecule; CCD, charge-coupled device; CG-1, Calcium Green-1; CGRP, calcitonin gene-related peptide; CICR, Ca^{2+} -induced Ca^{2+} release; DIC, differential interference contrast; DRG, dorsal root ganglion; FLIP, focal laser-induced photolysis; IgSF, immunoglobulin superfamily; MAG, myelin-associated glycoprotein; NP-EGTA, o-nitrophenyl EGTA; PKA, protein kinase A; RyR, ryanodine receptor.

step for identifying downstream Ca^{2+} effectors and understanding the precise mechanisms of growth cone navigation.

Whilst guided by molecular guidance cues, a migrating growth cone also makes adhesive contact with its environment via cell adhesion molecules (CAMs). CAMs expressed by neurons can be divided into three large families: integrins, cadherins, and the immunoglobulin superfamily (IgSF) members. Cadherins and the majority of IgSF CAMs interact homophilically, i.e., with the same type of molecules present on adjacent cells (Takeichi, 1991; Brummendorf and Rathjen, 1994). In contrast, integrins interact heterophilically, i.e., with extracellular matrix molecules, such as laminin (Letourneau et al., 1994). Upon ligand binding, different sets of CAMs expressed at the growth cone are likely to influence its turning response to guidance cues. For example, growth cone attraction to netrin-1 is converted to repulsion by laminin (Hopker et al., 1999). Furthermore, neuropilin-1 forms a cis-dimer with L1, an IgSF CAM, on the growth cone membrane and mediates repulsive turning against semaphorin 3A (Castellani et al., 2000). This repulsive response is converted to attraction by trans binding L1 with neuropilin-1 (Castellani et al., 2002). These results raise the possibility that CAMs influence the Ca^{2+} signals that mediate growth cone steering in response to guidance cues.

In this paper, we report two major findings: (1) the primary determinant of the turning direction is the source of Ca^{2+} influx to the growth cone cytosol. RyR-mediated CICR triggers attractive turning, whereas Ca^{2+} signals without CICR induce repulsive turning. Consistent with this *in vitro* result, the RyR is also implicated in axon guidance *in vivo*. (2) CAMs influence growth cone steering by regulating the RyR activity via cAMP and protein kinase A (PKA). Growth cones migrating on an L1 or N-cadherin substrate have active RyRs and make an attractive turn in response to Ca^{2+} signals, whereas growth cones on a laminin substrate show the opposite behavior. Our results indicate that axon-guiding and CAM-derived signals merge at the level of RyRs, which serve as key regulators of growth cone navigation.

Results

Ca^{2+} -induced growth cone turning on different substrates

Spatially restricted Ca^{2+} signals in a growth cone of a dorsal root ganglion (DRG) neuron were produced by focal laser-induced photolysis (FLIP) of a caged Ca^{2+} compound, *o*-nitrophenyl EGTA (NP-EGTA) compounded with Ca^{2+} in the cytosol. Time-lapse images of $[\text{Ca}^{2+}]_c$ using Calcium Green-1 (CG-1) demonstrated a focal and transient elevation of $[\text{Ca}^{2+}]_c$ in response to a single laser pulse that photolyzed NP-EGTA (Fig. 1 A). This type of experimental manipulation has been used extensively to study the physiological roles of Ca^{2+} signals in axon growth and guidance (Gomez and Spitzer, 1999; Gomez et al., 2001; Wen et al., 2004). Consistent with a previous study (Zheng, 2000), repetitive FLIP of NP-EGTA on one side of the growth cone resulted in attractive turning on both L1 and N-cadherin substrates (Fig. 1, B and D; and Fig. 2 A). The attractive turning was sometimes preceded by lamellipo-

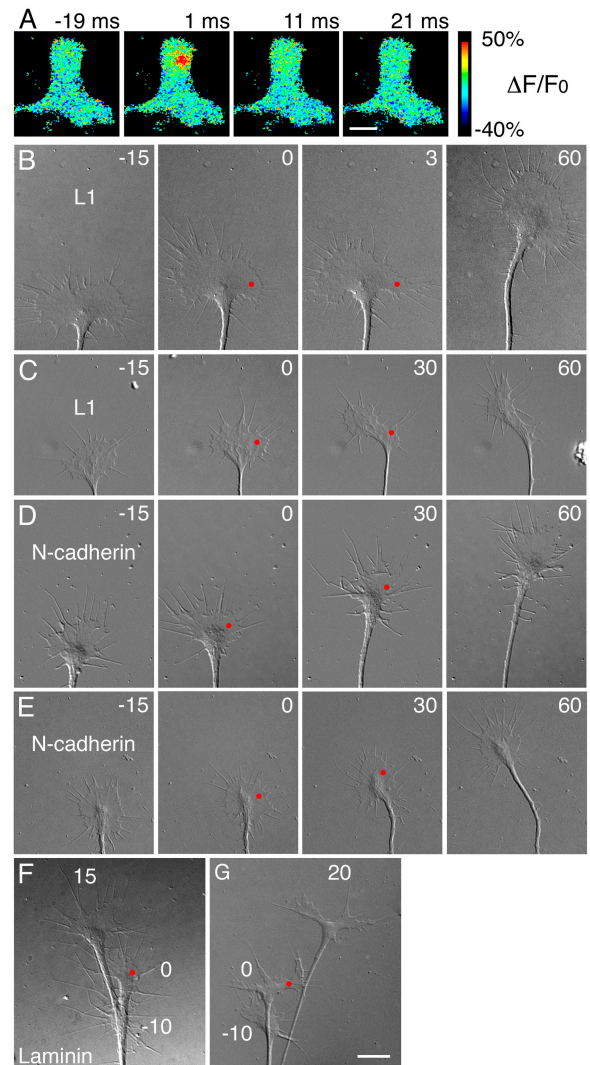


Figure 1. Ca^{2+} -induced growth cone turning on different substrates. (A) A localized and transient $[\text{Ca}^{2+}]_c$ elevation is produced by single FLIP of NP-EGTA in a chick DRG growth cone. Shown is the time course of the Ca^{2+} signal (CG-1 $\Delta F/F_0$ in pseudocolor). Each image was acquired by a 10-ms exposure starting at the indicated time point after the laser shot. Bar, 10 μm . Time-lapse DIC images showing Ca^{2+} -induced growth cone turning on L1 (B and C), N-cadherin (D and E), or laminin (F and G). Rp-cAMPS (C and E) or Sp-cAMPS (G) was added to the culture media. Loaded NP-EGTA in the growth cone was uncaged every 3 s by laser irradiation at the red spot. Digits represent minutes after the onset of repetitive FLIP. Growth cone images on laminin at different time points were superimposed (F and G). Bar, 10 μm .

dial protrusion (Fig. 1 B, 3 min) and filopodial elongation (not depicted), as reported previously (Lau et al., 1999; Cheng et al., 2002). In contrast, the same FLIP treatment caused repulsive turning on a laminin substrate (Fig. 1 F and Fig. 2 A). As a control, simultaneous loading of 1,2-bis(*o*-aminophenoxy)ethane-*N,N,N',N'*-tetraacetic acid (BAPTA), a fast Ca^{2+} chelator, completely negated the turning responses to NP-EGTA photolysis, indicating that Ca^{2+} released from NP-EGTA, but not byproducts of photolyzed NP-EGTA, was responsible for growth cone turning (Fig. 2 and see Fig. 7). These results indicate that, depending on the substrates, focal Ca^{2+} signals in growth cones induce either attractive or repulsive turning.

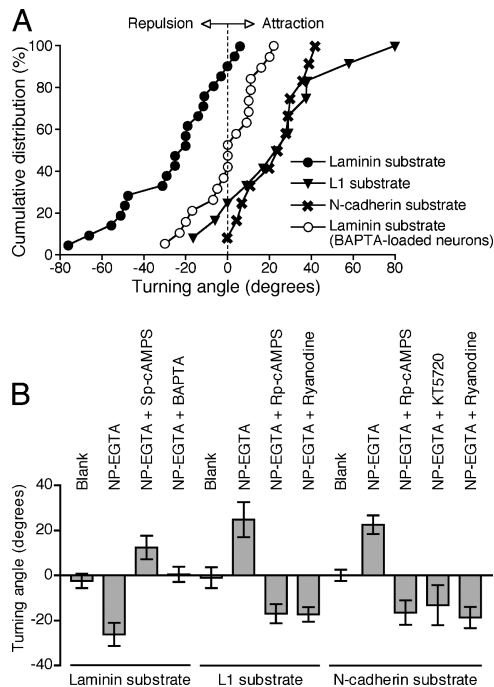


Figure 2. Involvement of cAMP and RyRs in Ca^{2+} -induced growth cone turning. (A) The distribution of turning angles of chick DRG growth cones on the three different substrates. Focal Ca^{2+} signals were produced on one side of the growth cones by repetitive FLIP of NP-EGTA. Each point represents the percentage of growth cones with turning angles equal to or smaller than that indicated on the abscissa. As a control, loading of BAPTA canceled FLIP-induced growth cone turning. (B) The average turning angles of growth cones on the three different substrates. Treatment of growth cones with the indicated drugs (Sp-cAMPS, Rp-cAMPS, ryanodine, or KT5720) reversed the turning responses to Ca^{2+} signals. Growth cones without NP-EGTA loading (blank) did not show a directional response to repetitive laser irradiation. Error bars represent 11–21 growth cones.

The three substrates (L1, N-cadherin, and laminin) did not influence the subpopulations of surviving neurons as shown in a previous study (Nishimura et al., 2003), excluding the possibility that the differential turning behavior of growth cones was dependent on neuronal cell types.

Substrate dependency of Ca^{2+} -induced growth cone turning is accounted for by differential cAMP activities

Hopker et al. (1999) previously reported that netrin-1-mediated attraction of retinal growth cones was converted to repulsion by laminin. These authors also explained that the amount of cAMP in growth cones, as assessed by immunocytochemistry, was decreased in the presence of laminin, suggesting that cAMP might mediate cross talk between growth cone guidance and adhesion. Therefore, we first compared cAMP levels in DRG neurons cultured on three different substrates—L1, N-cadherin, and laminin. A competitive immunoassay showed that the neurons contained higher cAMP levels on L1 and N-cadherin than on laminin (Fig. 3 A). To quantify the activity of cAMP in the growth cone, we used FICRHR, which changes the efficiency of fluorescence resonance energy transfer from fluorescein to rhodamine, in response to cAMP binding to the PKA regulatory subunits (Adams et al., 1991). Consistent with

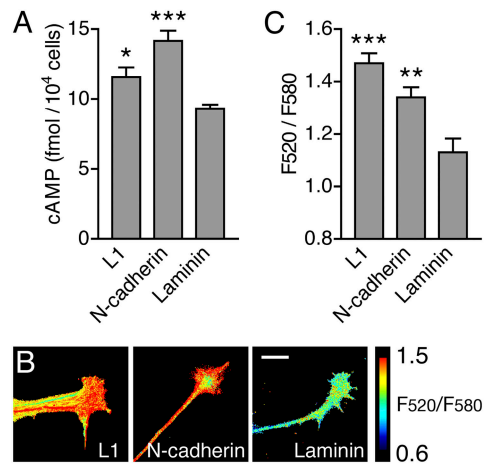


Figure 3. CAMs regulate cAMP activities in growth cones. (A) Competitive immunoassays showing intracellular cAMP levels in chick DRG neurons on L1, N-cadherin, or laminin. *, $P < 0.05$; ***, $P < 0.001$; compared with a laminin substrate ($n = 7$). (B) FICRHR ratio images (F_{520}/F_{580} in pseudocolor) showing cytosolic cAMP activities in chick DRG growth cones on L1, N-cadherin, or laminin. Bar, 10 μ m. (C) Measurements of cAMP activities in growth cones on the three different substrates. The F_{520}/F_{580} values of FICRHR were averaged in growth cones. Error bars represent 26–32 growth cones. **, $P < 0.01$; ***, $P < 0.001$; compared with a laminin substrate.

our immunoassay data, the ratio images (F_{520}/F_{580}) showed that the cAMP activities in the growth cones were higher on L1 and N-cadherin than on laminin (Fig. 3, B and C). Next, the effect of cAMP modulation on Ca^{2+} -induced growth cone turning was examined. Bath application of Rp-cAMPS, a membrane-permeable cAMP antagonist, converted Ca^{2+} -induced attraction to repulsion on both L1 and N-cadherin substrates (Fig. 1, C and E; and Fig. 2 B). An inhibition of PKA, a cAMP-dependent protein kinase, by KT5720 had a similar result (Fig. 2 B). Sp-cAMPS, a cAMP agonist that activates PKA, converted Ca^{2+} -induced repulsion to attraction on laminin (Fig. 1 G and Fig. 2 B). These results indicate that differential cAMP–PKA activities account for the substrate dependency of Ca^{2+} -induced growth cone turning, with high cAMP–PKA activities favoring attraction and low cAMP–PKA activities causing repulsion.

Because PKA has been shown to phosphorylate RyRs and facilitate CICR in other biological systems (Yoshida et al., 1992; Valdivia et al., 1995; Wehrens and Marks, 2003), we assessed whether Ca^{2+} -induced growth cone attraction depended also on RyR-mediated CICR in addition to cAMP–PKA. As shown in Fig. 2 B, Ca^{2+} signals caused growth cone repulsion even on L1 and N-cadherin substrates if neurons were pretreated with a high dose (100 μ M) of ryanodine to trap RyRs in the closed state (Zucchi and Ronca-Testoni, 1997), suggesting that RyRs cooperated with cAMP–PKA in Ca^{2+} -mediated growth cone attraction.

cAMP facilitates RyR-mediated CICR in growth cones

To test whether cAMP–PKA facilitated CICR in growth cones, we analyzed the amplitude of Ca^{2+} signals by CG-1 imaging synchronized with FLIP. Focal $[Ca^{2+}]_c$ was quantified by averaging CG-1 $\Delta F/F_0$ within a 2- μ m-diameter zone centered by

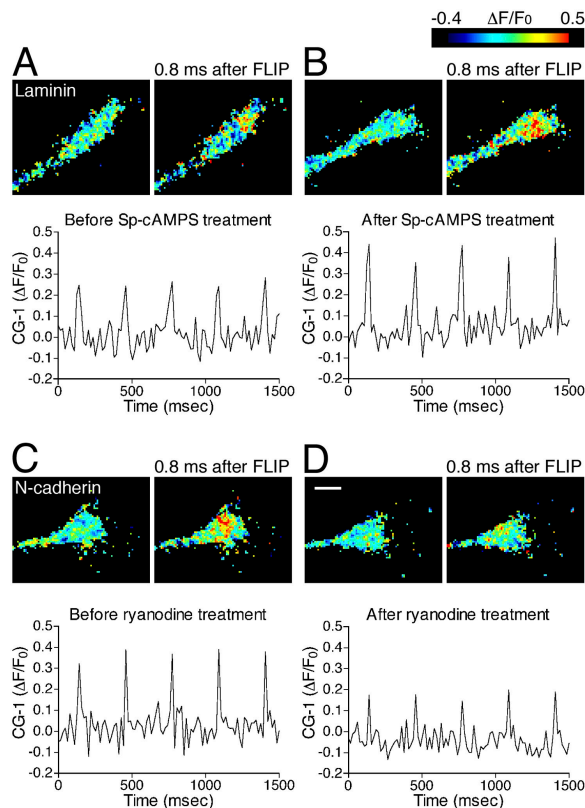


Figure 4. Pharmacological dissection of different components of Ca^{2+} signals induced by NP-EGTA photolysis. (A and B) Sp-cAMPS augments FLIP-induced Ca^{2+} signals in a chick DRG growth cone on laminin. Before and after a 5-min treatment with Sp-cAMPS (A and B, respectively), the Ca^{2+} signals were analyzed in the same growth cone under the same FLIP conditions. CG-1 fluorescence was imaged at the exposure of 15.7 ms. The pseudocolor images show $\Delta\text{F}/\text{F}_0$ immediately before or 0.8 ms after single FLIP. The $\Delta\text{F}/\text{F}_0$ values were averaged within a 2- μm -diam zone centered by the FLIP site and plotted as a function of time. The graphs show five Ca^{2+} elevations ($\Delta\text{F}/\text{F}_0$ spikes) induced by five laser pulses at 300-ms intervals. Note that the amplitude of the Ca^{2+} signals is augmented by the Sp-cAMPS treatment (compare A and B). (C and D) A high dose of ryanodine attenuates FLIP-induced Ca^{2+} signals in a growth cone on N-cadherin. The amplitude of Ca^{2+} signals was analyzed in the same growth cone before and after a 5-min treatment with 100 μM ryanodine (C and D, respectively), using experimental methods described in A and B. Bar, 5 μm .

the FLIP site (Fig. 4). A transient elevation of $[\text{Ca}^{2+}]_c$ was observed only in the first charge-coupled device (CCD) frame after FLIP (0.8–16.5 ms after a laser pulse; see Materials and methods). This elevation should be the sum of Ca^{2+} liberation from NP-EGTA and secondary Ca^{2+} influx to the cytosol, if applicable. To dissect the two different Ca^{2+} sources, we compared the amplitude of $[\text{Ca}^{2+}]_c$ elevations in the same growth cones before and after pharmacological treatments. In a growth cone on laminin, for example, a train of five laser pulses produced Ca^{2+} signals of similar amplitude that increased after treating the growth cone with Sp-cAMPS (Fig. 4, A and B). In contrast, Ca^{2+} -signal amplitude decreased after a growth cone on N-cadherin was treated with 100 μM ryanodine (Fig. 4, C and D). The amplitude of five Ca^{2+} elevations ($\Delta\text{F}/\text{F}_0$ spikes) after five laser pulses was averaged and compared in the same growth cone before and after a 5-min treatment with various

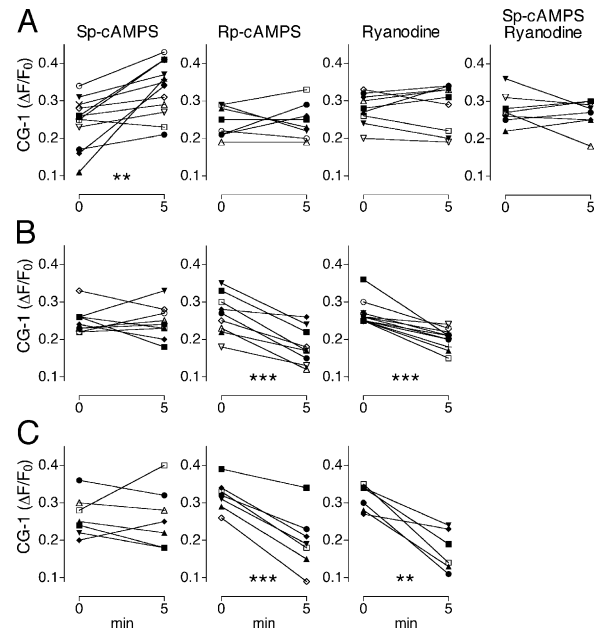


Figure 5. CAMs influence RyR-mediated CICR via cAMP. The effects of the indicated drugs on FLIP-induced Ca^{2+} signals were analyzed in chick DRG growth cones on laminin (A), L1 (B), or N-cadherin (C). As exemplified in Fig. 4, the amplitude of $\Delta\text{F}/\text{F}_0$ spikes was defined as $\Delta\text{F}/\text{F}_0$ values averaged within a 2- μm -diam zone immediately after FLIP. The amplitude of five $\Delta\text{F}/\text{F}_0$ spikes induced by five laser pulses at 300-ms intervals was averaged and plotted as the ordinate. The abscissa indicates the minutes after an application of Sp-cAMPS, Rp-cAMPS, and/or ryanodine. Each line represents a drug-induced change of the Ca^{2+} -signal amplitude in a single growth cone. Datasets with statistically significant changes are marked by asterisks. **, $P < 0.01$; ***, $P < 0.001$; paired t test.

pharmacological reagents (Fig. 5). The Sp-cAMPS treatment augmented Ca^{2+} signals in growth cones only on a laminin substrate, presumably because the downstream cascade of cAMP was fully active on L1 and N-cadherin, even in the absence of Sp-cAMPS. This augmentation by Sp-cAMPS on laminin was abolished by a simultaneous treatment with 100 μM ryanodine, suggesting that Sp-cAMPS facilitated an additional increase of $[\text{Ca}^{2+}]_c$ via ryanodine-sensitive channels, such as RyR-mediated CICR. Consistent with this idea, the treatment with either Rp-cAMPS or ryanodine attenuated Ca^{2+} signals in growth cones on L1 and N-cadherin but not on laminin.

Among the three RyR isoforms (types 1, 2, and 3), only the type 3 isoform (RyR3) has been detected in DRGs by Western blotting (Lokuta et al., 2002). Therefore, we analyzed DRG neurons derived from RyR3 knockout mice (Futatsugi et al., 1999) to further confirm that the RyR is involved in the augmentation of Ca^{2+} signals induced by cAMP. As reviewed by Bouchard et al. (2003), there has been accumulating evidence for the presence of functional RyRs in the axons and presynaptic terminals. Our immunocytochemical analysis showed the punctate distribution of RyRs in growth cones with strong expression in the central domain and weak expression in the lamellipodia (Fig. 6, A, B, D, and E). RyR expression and distribution were not influenced by culture substrates (unpublished data). Although the primary antibody recognized all three RyR isoforms (Kuwajima et al., 1992; Futatsugi et al.,

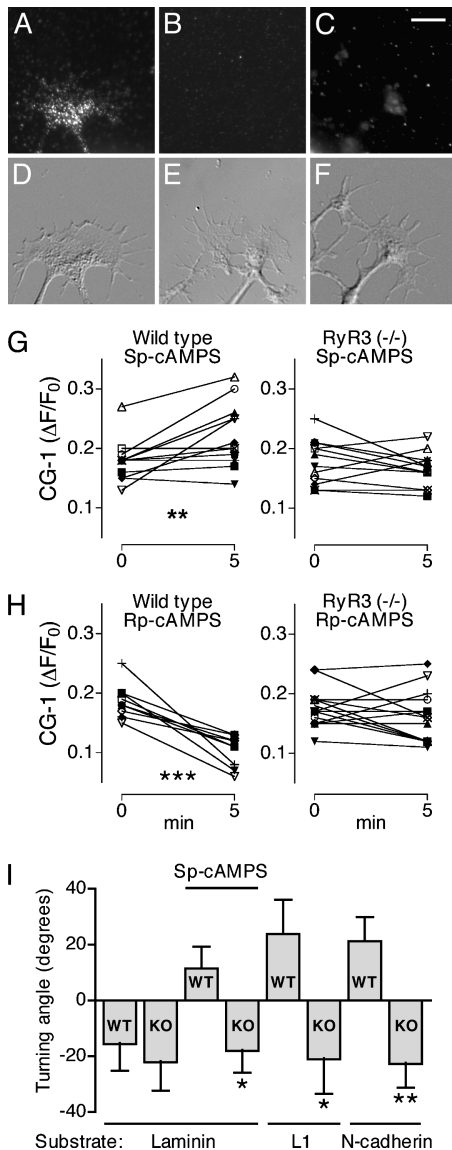


Figure 6. Ca^{2+} signals and turning directions of RyR3-deficient growth cones. (A–F) Immunocytochemistry of RyRs in mouse DRG neurons. RyRs in wild-type (A and D) or RyR3-deficient (C and F) growth cones were labeled with an antibody that recognized all three isoforms. As a control, the primary antibody was omitted from the labeling procedure on wild-type growth cones (B and E). Shown are RyR immunofluorescence (A–C) and DIC images (D–F). Bar, 10 μm . (G and H) FLIP-induced Ca^{2+} signals in wild-type and RyR3-deficient growth cones. As described in Fig. 5, the effects of drugs (Sp-cAMPS or Rp-cAMPS) on the $\Delta\text{F}/\text{F}_0$ spike amplitude were analyzed in growth cones on laminin (G) or L1 (H). Each line represents a drug-induced change of the amplitude in a single growth cone. Datasets with statistically significant changes are marked by asterisks. **, $P < 0.01$; ***, $P < 0.001$; paired t test. (I) The average turning angles of wild-type (WT) or RyR3-knockout (KO) growth cones on the three different substrates. As indicated, some growth cones were analyzed in the presence of Sp-cAMPS. Error bars represent 9–15 growth cones. *, $P < 0.05$; **, $P < 0.01$; compared with wild-type growth cones under the same culture conditions.

1999), the immunoreactivity to this antibody was reduced or sometimes absent in RyR3-deficient growth cones (Fig. 6, C and F), further confirming that RyR3 is a predominant isoform in DRG neurons. On a laminin substrate, the Sp-cAMPS treatment augmented the amplitude of FLIP-induced Ca^{2+} signals

in wild-type growth cones, whereas the same Sp-cAMPS treatment did not have that effect in RyR3-deficient growth cones (Fig. 6 G). On L1, the Rp-cAMPS treatment attenuated the amplitude of Ca^{2+} signals in wild-type growth cones but not in RyR3-deficient growth cones (Fig. 6 H). Collectively, our results indicate that the growth cone regulates the efficiency of RyR3-mediated CICR through cAMP–PKA upon contact with different substrates.

RyR3 controls Ca^{2+} -mediated turning of growth cones

Our results up to this point suggested that cAMP–PKA controlled Ca^{2+} -induced turning of growth cones by modulating the efficiency of RyR3-mediated CICR. Therefore, we next performed the axon turning assay using RyR3-deficient neurons. On L1 and N-cadherin substrates that activated the cAMP pathway, RyR3-deficient growth cones showed Ca^{2+} -mediated repulsion, whereas wild-type growth cones exhibited attraction (Fig. 6 I). The most important evidence for the involvement of RyR3 downstream of the cAMP pathway came from the assay on a laminin substrate, in which Ca^{2+} -mediated repulsion of wild-type growth cones, but not of RyR3-deficient growth cones, was converted to attraction by Sp-cAMPS (Fig. 6 I). Collectively, growth cone–substrate interactions regulate cAMP-activated RyR3-mediated CICR that determines the turning response to Ca^{2+} signals.

Because RyR-mediated CICR augmented the amplitude of FLIP-induced Ca^{2+} signals (Fig. 5), it remained to be determined whether the turning behavior of growth cones depended on the amplitude or the source of Ca^{2+} signals. Therefore, we tested whether attractive turning of growth cones could be switched to repulsion when the Ca^{2+} -signal amplitude was lowered by coloaded neurons with NP-EGTA and increasing concentrations of BAPTA followed by laser irradiation (Fig. 7). Elevating BAPTA acetoxymethyl ester (AM) concentrations caused attenuated or undetectable Ca^{2+} signals (CG-1 $\Delta\text{F}/\text{F}_0$) in growth cones on N-cadherin and decreased the attractive turning angle to zero without causing a significant repulsive turn. This result indicated that lowering the amplitude of Ca^{2+} signals was not sufficient to induce growth cone repulsion if the cAMP–PKA pathway was active. We also tested whether growth cone repulsion on laminin could be converted to attraction by increasing the Ca^{2+} -signal amplitude. Previous work demonstrated that FLIP-induced Ca^{2+} signals in the growth cones of *Xenopus laevis* spinal neurons on laminin caused attractive or repulsive turning when the growth cones had been loaded with 6 or 2 μM NP-EGTA, respectively (Wen et al., 2004). However, under our experimental conditions, wild-type mouse DRG growth cones on laminin still showed repulsive turning ($-13.3 \pm 7.4^\circ$, $n = 11$) even if loaded with the high concentration (6 μM) of NP-EGTA followed by FLIP. This result was further confirmed with RyR3-deficient growth cones on N-cadherin. In this set of experiments, wild-type and RyR3-deficient growth cones were loaded with 2 and 6 μM NP-EGTA, respectively. The baseline $[\text{Ca}^{2+}]_i$ in the growth cones was measured by Fura-2 ratio imaging, and the amplitude of $[\text{Ca}^{2+}]_i$ elevations immediately after FLIP was determined by

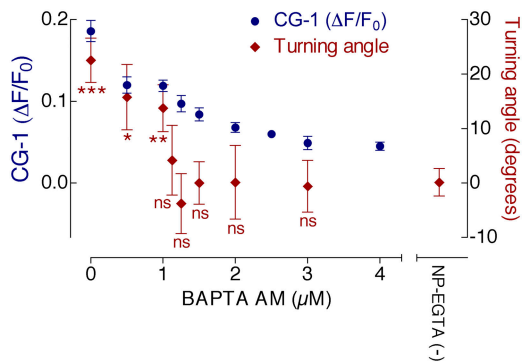


Figure 7. The relationship between the Ca²⁺-signal amplitude and growth cone turning. The amplitude of FLIP-induced Ca²⁺ signals was controlled by preloading chick neurons with increasing concentrations of BAPTA. Blue dots indicate the mean amplitude of ΔF/F₀ spikes that was calculated as described in Fig. 5. Each dot involves 6–10 growth cones. Red diamonds indicate the mean turning angles, each involving 8–13 growth cones. *, P < 0.05; **, P < 0.01; ***, P < 0.001; compared with the turning angles of growth cones that were not loaded with NP-EGTA.

CG-1 single-wavelength measurements as described previously (Lev-Ram et al., 1992). The baseline [Ca²⁺]_c in wild-type growth cones was 202 ± 17 nM (n = 50), which rose to 643 ± 48 nM (n = 8) after FLIP. Similarly, [Ca²⁺]_c in RyR3-deficient growth cones rose from 207 ± 12 nM (n = 51) to 861 ± 106 nM (n = 11) in response to FLIP. Statistical analysis showed no significant difference between the two groups of growth cones, indicating that the Ca²⁺-signal amplitude in RyR3-deficient growth cones with 6 μM NP-EGTA loading was equivalent to or slightly higher than that in wild-type growth cones with 2 μM NP-EGTA loading. Then, the two groups were tested for their turning response to FLIP-induced Ca²⁺-signals. RyR3-deficient growth cones with 6 μM NP-EGTA exhibited repulsive turning (−14.6 ± 8.1°, n = 10), whereas wild-type growth cones with 2 μM NP-EGTA showed attraction (26.5 ± 8.6°, n = 7) in parallel experiments. The difference was statistically significant (P < 0.05). This result indicated that, depending on the occurrence of RyR3-mediated CICR, growth cones were either attracted or repelled by [Ca²⁺]_c elevations of the equivalent amplitude on top of the same baseline level. We conclude that the source of Ca²⁺ influx, rather than its amplitude or the baseline Ca²⁺ level, is a decisive factor that regulates the direction of growth cone steering: RyR3-mediated CICR triggers attraction, whereas Ca²⁺ signals without CICR induce repulsion.

RyR3 is implicated in DRG axon guidance in vivo

To test for the involvement of RyRs in growth cone steering in vivo, we analyzed DRG axon trajectories in the spinal cord of RyR3 knockout mice. Because our in vitro experiments were performed using DRG neuronal cultures supplemented with NGF, the corresponding subpopulation of DRG axons in vivo was labeled by an antibody against calcitonin gene-related peptide (CGRP), a marker for the NGF-dependent TrkA-positive nociceptive neurons (Snider, 1994; Averill et al., 1995). As reported previously (Gibson et al., 1984), there are two major

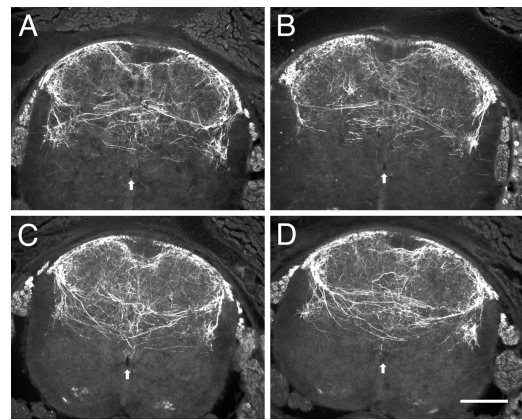


Figure 8. CGRP-positive axon trajectories in the spinal cords. Nociceptive DRG axons were labeled by CGRP immunofluorescence. Shown are transverse sections of the spinal cord at the fifth lumbar segment from wild-type (A and B) or RyR3-knockout (C and D) mice. Dorsal is uppermost, and the arrows indicate the central canal. Bar, 200 μm.

types of CGRP-positive axon projections in the spinal cord: those that terminate in the superficial dorsal horn (laminae I and II) and those that project deeply in the dorsal gray commissure (dorsal to the central canal; Fig. 8). Although the CGRP-positive superficial projections were not affected by RyR3 deficiency, we found a significant difference in the deep projections between wild-type and RyR3 knockout mice. In the wild-type spinal cord, CGRP-positive axons projecting toward the dorsal gray commissure extended horizontally or in a slightly dorsal trajectory away from the central canal (Fig. 8, A and B). In the RyR3-deficient spinal cord, however, the axons projected ventrally toward the central canal (Fig. 8, C and D). This phenotype was consistently observed in six knockout animals in comparison with six wild-type littermates. The similar pathfinding error of nociceptive axons was observed when the spinal cord was treated with a function-blocking antibody against NgCAM (a chick homologue of L1) or its binding partner, axonin-1 (Perrin et al., 2001), suggesting that homophilic or heterophilic L1 interactions are required for these axons to be guided correctly by extracellular cues.

Discussion

During development, the precise pattern of neuronal networks depends on the guided advance of growth cones along correct paths toward their targets. The growth cone serves as the sensory and motile apparatus for translating extracellular cues into directional elongation of the axon. A cytosolic Ca²⁺ signal is one of the most important messengers that relay extracellular information to the motile behavior of growth cones (Davenport et al., 1993; Kuhn et al., 1998; Takei et al., 1998; Gomez and Spitzer, 1999; Doherty et al., 2000; Gomez et al., 2001; Tang et al., 2003). Elongating axons could respond to the cytosolic Ca²⁺ signal in multiple ways, depending on the source of Ca²⁺ influx to the cytosol and its amplitude and frequency. The work we present here demonstrates the importance of the source of Ca²⁺ signals in determining the turning direction of growth cones, in which RyR-mediated CICR trig-

gers attraction, whereas Ca^{2+} signals without CICR induce repulsion. We also show that CAMs regulate RyR activity through cAMP and PKA and that the growth cone is able to change its turning behavior on different substrates. The most significant point of our work is the direct demonstration, using gene-manipulated mice, that RyR3 is a downstream component of the cAMP–PKA pathway and that RyR3 controls the bidirectional turning responses induced by Ca^{2+} signals of the same polarity in growth cones. In this way, axon-guiding and CAM-derived signals are integrated at the level of RyR3, which may provide growth cones with the flexibility of generating distinct responses to the same guidance cue in different environmental situations *in vivo*. This concept has been supported by our experiment that showed the altered projection of DRG axons in the RyR3-deficient spinal cord, although axon-guiding molecules involved in this phenotype remain to be identified. Antibody perturbation experiments by Perrin et al. (2001) suggested that impaired L1 interactions with its binding partners caused a similar guidance error of DRG axons, which is consistent with our concept that L1 controls growth cone turning responses to guidance cues by modifying cytosolic Ca^{2+} signals.

Because the occurrence of CICR and the amplitude of Ca^{2+} signals are tightly associated, it has been challenging to dissect these two factors experimentally. Although our data support the idea that the source of Ca^{2+} signals is the primary determinant of the turning direction of growth cones, several previous studies have suggested that the Ca^{2+} -signal amplitude is the important factor. For example, Henley et al. (2004) conducted clever experiments in which different levels of $[\text{Ca}^{2+}]_c$ gradients were created across a growth cone by unilateral application of a Ca^{2+} -selective ionophore through a micropipette in the presence of distinct preset Ca^{2+} concentrations in bathing media. Their study showed that high- or low-amplitude Ca^{2+} signals were sufficient to trigger attraction or repulsion of the growth cone, respectively. In their experiments, however, low-amplitude Ca^{2+} signals were produced after treating the cells with thapsigargin that depleted Ca^{2+} from the internal stores, raising the possibility that impaired CICR might have been responsible for the repulsion. Another example comes from studies by Zheng and colleagues (Zheng, 2000; Wen et al., 2004), in which they lowered the absolute level of cytosolic Ca^{2+} signals by removing Ca^{2+} from external bathing media. The growth cone repulsion observed under this experimental condition might have been attributable to the indirect depletion of internal Ca^{2+} stores. Therefore, the results in these two papers do not contradict our proposal that RyR-mediated CICR triggers attraction, whereas Ca^{2+} signals without CICR induce repulsion. A study by Henley et al. (2004) showed that MAG-induced growth cone repulsion was blocked by inhibiting Ca^{2+} influx from ryanodine-sensitive channels but not from plasmalemmal channels. Furthermore, Nishiyama et al. (2003) reported that netrin-1–induced attraction was associated with high-amplitude Ca^{2+} influx through plasmalemmal L-type channels. These results initially appear to be in conflict with our conclusions; however, we used a direct $[\text{Ca}^{2+}]_c$ elevation approach that bypassed activation of the

MAG or netrin-1 receptors on the plasma membrane and could avoid cross talk among different intracellular signals. Therefore, growth cone turning assayed by extracellular application of guidance molecules cannot be compared simply with our study that focuses on $[\text{Ca}^{2+}]_c$ elevations and their downstream events. We propose that Ca^{2+} -signal localization at the molecular level is a decisive factor for switching the steering direction of growth cones. Perhaps Ca^{2+} signals confined to nanodomains/microdomains activate distinct sets of molecular targets (Augustine et al., 2003), depending on the location of open Ca^{2+} channels as well as on the distance between these channels and Ca^{2+} -binding proteins. Although recent papers have identified some of the downstream effectors of Ca^{2+} (Robles et al., 2003; Wen et al., 2004), much more work will need to be done to understand the whole picture of switch-like mechanisms that navigate the growth cone bidirectionally in response to Ca^{2+} signals of different localization and amplitude.

Another important question concerns the causal relationship between cAMP–PKA and Ca^{2+} signals. Wen et al. (2004) demonstrated that the cAMP pathway acts downstream of $[\text{Ca}^{2+}]_c$ elevations, negatively regulating the repulsive signaling cascade that involves calcineurin and phosphatase-1. This inhibition by cAMP allows $[\text{Ca}^{2+}]_c$ elevations to activate only the attractive signaling components, thereby switching growth cone repulsion to attraction. In contrast, the cAMP pathway acts upstream of Ca^{2+} signals in growth cones guided by netrin-1 or MAG. Activation of the cAMP pathway increases the basal $[\text{Ca}^{2+}]_c$ in growth cones, which converts MAG-induced repulsion to attraction because MAG-induced $[\text{Ca}^{2+}]_c$ elevations can be superimposed on top of the higher basal $[\text{Ca}^{2+}]_c$ (Henley et al., 2004). Also, growth cone attraction by netrin-1 depends on L-type Ca^{2+} channel activation by cAMP–PKA (Nishiyama et al., 2003). The present study has demonstrated that the cAMP pathway activates RyRs and allows primary $[\text{Ca}^{2+}]_c$ elevations to induce the secondary Ca^{2+} influx from the internal stores, thereby acting at the level of Ca^{2+} signaling. Although the cAMP pathway may exert multiple roles at multiple steps in signal transduction cascades, we believe that the major mode of cAMP action, at least in DRG growth cones, is on the RyR-mediated CICR because RyR3-deficient axons did not respond to cAMP activation in either the Ca^{2+} imaging (Fig. 6 G) or the turning assay (Fig. 6 I).

In summary, this study shows that CAMs control Ca^{2+} -mediated steering of growth cones via cAMP and RyRs. Upon contact with differing extracellular environments, growth cones could change their turning responses to axon guidance cues by modulating the efficiency of RyR-mediated CICR. In this way, CAMs and axon-guiding molecules cooperate to navigate axons along their correct paths. Because activating cAMP pathways has been shown to overcome myelin-associated inhibitors of axon regeneration (e.g., MAG) in the damaged central nervous system (Cai et al., 1999; Neumann et al., 2002; Qiu et al., 2002), our findings further suggest that CAMs may play a role in regenerating axons, presumably through a mechanism similar to that used by cAMP-dependent switching of growth cone repulsion to attraction.

Materials and methods

Cell culture

DRGs dissected from embryonic day 9 chicks or postnatal day 0 mice were dissociated as previously described (Nakai and Kamiguchi, 2002) and plated on a glass-based dish coated with 9 $\mu\text{g}/\text{cm}^2$ laminin (Life Technologies) or CAM-Fc chimeric proteins that consisted of the whole extracellular domain of a CAM (L1 or N-cadherin) and the Fc region of human IgG. The L1-Fc cDNA construct was provided by Dr. Vance Lemmon (University of Miami, Miami, FL), and the N-cadherin-Fc construct by Dr. Patrick Doherty (King's College London, London, UK). Production of CAM-Fc and preparation of CAM-Fc-coated dishes were performed as described previously (Kamiguchi and Yoshihara, 2001). The neuronal cultures were maintained in Leibovitz's L-15 medium (Life Technologies) supplemented with N-2 (Life Technologies), 50 ng/ml NGF (Promega), and 750 $\mu\text{g}/\text{ml}$ BSA (Life Technologies) in a humidified atmosphere of 100% air at 37°C.

FLIP setup

The 355-nm Nd:YAG laser beam (a pulse width of 5 ns; New Wave Research) was introduced into an inverted microscope (TE300; Nikon) through the random-scanning photolysis system (Hamamatsu Photonics) and was focused on a growth cone using a 100 \times Plan Fluor (NA 1.3, oil objective). Spatial restriction of FLIP (~ 1 μm in diam in the xy plane and ~ 2 μm in thickness in the z direction) was demonstrated by irradiating caged fluorescein maleimide (Dojindo) immobilized in acrylic polymer.

Growth cone turning assay

DRG neurons were incubated, unless otherwise noted, with 2 μM NP-EGTA AM (Invitrogen) and 0.025% Cremophor EL (Sigma-Aldrich) for 30 min and then washed. After an additional 1.5-h incubation, an area within a lamellipodium in one side of the growth cone was irradiated with a laser (~ 35 nJ/pulse) every 3 s while time-lapse differential interference contrast (DIC) images of the growth cone were acquired with a CCD camera. Growth cone turning was assessed by tracing the middle point of the distal edge of the growth cone central domain. On L1 and N-cadherin substrates, the original (preFLIP) direction of axon extension was defined as a straight line connecting the positions of the growth cone at the onset and 15 min before the onset of FLIP. The direction during FLIP was defined as a straight line connecting the positions of the growth cone at the onset and at the end of repetitive FLIP for 60 min. The growth cone turning angle was defined by the angle between the original direction and the direction during FLIP. Because axons extended faster on a laminin substrate, the turning angle on laminin was determined using the positions of the growth cone at 10 min before, at the onset of, and at 30 min after repetitive FLIP. Included in this assay were only those growth cones with net extension >5 μm during the preFLIP periods and without collapse during the time-lapse imaging.

In some experiments, various concentrations of BAPTA AM (Invitrogen) were loaded into neurons before the turning assay (a 20-min incubation with BAPTA AM and Cremophor EL followed by a 30-min incubation). The following reagents were applied to some cultures 30 min before the turning assay: 20 μM Sp-cAMPS (Calbiochem), 20 μM Rp-cAMPS (Calbiochem), 100 μM ryanodine (Calbiochem), and 100 nM KT5720 (Calbiochem).

Imaging FLIP-induced Ca^{2+} signals

Dextran (10,000 D) conjugated with CG-1 (3 mg/ml; Invitrogen) was introduced into DRG neurons by trituration loading as described previously (Sydor et al., 1996). After NP-EGTA loading, FLIP-induced Ca^{2+} signals were imaged with a high-speed CCD camera (HiSCA; Hamamatsu Photonics) coupled with a Gen IV image intensifier (Hamamatsu Photonics). The images were background subtracted and expressed as the change in CG-1 fluorescence relative to the baseline before FLIP ($\Delta F/F_0$) using the AquaCosmos software version 2.0 (Hamamatsu Photonics). Each image was acquired by a 15.7-ms exposure with CCD binning set at 2×2 . The sampling rate was 63.7 Hz. To synchronize FLIP with CG-1 imaging, a laser shot was triggered by a transistor-transistor logic signal that was generated by AquaCosmos and controlled in timing by a pulse generator (Nihon Kohden). Typically, a CCD exposure was initiated 0.8 ms after the laser shot (~ 90 nJ/pulse). This interval was sufficiently long to prevent laser-induced autofluorescence from affecting the CG-1 image. Focal Ca^{2+} signals were evaluated by averaging $\Delta F/F_0$ values within a 2- μm -diam zone centered by the FLIP site. After a 5-min incubation with 20 μM Sp-cAMPS, 20 μM Rp-cAMPS, and/or 100 μM ryanodine, FLIP-induced Ca^{2+} signals were again analyzed in the same growth cone under the same experimental conditions.

In some experiments, FLIP-induced Ca^{2+} signals were quantified by converting the CG-1 $\Delta F/F_0$ value to $[\text{Ca}^{2+}]$ using the following formula (Lev-Ram et al., 1992): $[\text{Ca}^{2+}] = ([\text{Ca}^{2+}]_{\text{rest}} + K_d \times f/f_{\text{max}})/(1 - f/f_{\text{max}})$, where $f = \Delta F/F_0$ and $f_{\text{max}} = \Delta F_{\text{max}}/F_0$. The dissociation constant (K_d) of dextran-conjugated CG-1 was determined as 413 nM (37°C, pH 7.2) by using the calcium calibration buffer kit with magnesium #2 (Invitrogen). The resting Ca^{2+} concentration ($[\text{Ca}^{2+}]_{\text{rest}}$) was measured by Fura-2 ratio imaging as described in the next section. The ΔF_{max} was the maximal change of CG-1 fluorescence, which was determined in every growth cone by applying 10 μM of calcium ionophore A23187 (Sigma-Aldrich) in media with a saturating amount of Ca^{2+} (1.26 mM).

Fura-2 ratio imaging

DRG neurons were incubated with 2 μM Fura-2 AM (Invitrogen) and 0.025% Cremophor EL for 30 min. After an additional 1-h incubation, Fura-2 was excited at two wavelengths (340 and 380 nm), and emission images were acquired at 510 nm. After background subtraction, the ratio of fluorescence intensity ($R = F_{340}/F_{380}$) was measured in a growth cone and converted to $[\text{Ca}^{2+}]$ using the following standard formula (Grynkiewicz et al., 1985): $[\text{Ca}^{2+}] = K_d \times (F_{\text{free}}/F_{\text{bound}}) \times (R - R_{\text{min}})/(R_{\text{max}} - R)$. The dissociation constant (K_d) of Fura-2 was determined as 207 nM (37°C, pH 7.2) by using the calcium calibration buffer kit with magnesium #2 (Invitrogen). The constant $F_{\text{free}}/F_{\text{bound}}$ was the fluorescence ratio of the Ca^{2+} -free and -saturated forms of Fura-2 upon 380-nm excitation. R_{min} designated the minimum R measured in the absence of Ca^{2+} , and R_{max} the maximum R at a saturating Ca^{2+} concentration. These parameters were determined in growth cones by applying 10 μM A23187 in media with a saturating amount of Ca^{2+} (1.26 mM) followed by perfusion with Ca^{2+} -free buffer containing 2 mM EGTA. Values for $F_{\text{free}}/F_{\text{bound}}$, R_{min} , and R_{max} were 2.15, 0.32, and 4.12, respectively.

cAMP measurements

Intracellular cAMP levels in neurons were measured using a competitive nonacetylation immunoassay kit (GE Healthcare), according to the manufacturer's instructions.

We used fluorescence ratio imaging of FICRHR to measure the activity of cAMP in the growth cone cytosol. FICRHR (20 ± 5 μM ; Invitrogen) was pressure-injected into a DRG neuron with a micropipette. After 3 h of incubation, FICRHR was excited using a band-pass filter (484/15 nm), and two single-wavelength emission images (F_{520} and F_{580}) were simultaneously acquired using a band-pass (520/30 nm) and a log-pass filter (570 nm), respectively. After background subtraction, the ratio of F_{520}/F_{580} was calculated and averaged within the growth cone using AquaCosmos.

RyR immunocytochemistry

DRG neurons were fixed with 4% formaldehyde in PBS for 40 min, permeabilized and blocked with 0.1% Triton X-100 and 10% horse serum in PBS for 1 h, and then incubated with rabbit polyclonal anti-RyR antibody (anti-C2; 2 $\mu\text{g}/\text{ml}$; Kuwajima et al., 1992) overnight at 4°C. Primary antibody binding was detected using Alexa 488-conjugated goat anti-rabbit IgG secondary antibody (10 $\mu\text{g}/\text{ml}$; Invitrogen).

CGRP immunohistochemistry

Postnatal day 0 mice were deeply anesthetized and perfused with 4% formaldehyde in 0.1% Na-phosphate buffer. The lumbar spinal cord was dissected, postfixed overnight in the same fixative at 4°C, and infiltrated overnight with 25% sucrose in PBS at 4°C. 16- μm -thick cryostat sections were collected and stored at -20°C . After blocking and permeabilization with 10% horse serum and 0.1% Triton X-100 in PBS, the sections were incubated sequentially with rabbit polyclonal anti-CGRP antiserum (1:5,000 dilution; overnight at 4°C; Sigma-Aldrich) and Alexa 488-conjugated goat anti-rabbit IgG (10 $\mu\text{g}/\text{ml}$).

Statistics

Data were expressed as the mean \pm SEM. Statistical analyses were performed using Prism version 3.0a (GraphPad Software). Unless otherwise noted, a comparison between two groups was performed by an unpaired *t* test and a comparison among three or more groups by a one-way analysis of variance followed by Tukey's posttest. P values <0.05 were judged statistically different.

We would like to thank Dr. Vance Lemmon for providing us with the L1-Fc construct and Dr. Patrick Doherty for the N-cadherin-Fc construct.

This study was partially supported by a Grant-in-Aid for Scientific Research (C) of the Japan Society for the Promotion of Science (16500210) to H. Kamiguchi.

References

- Adams, S.R., A.T. Harootunian, Y.J. Buechler, S.S. Taylor, and R.Y. Tsien. 1991. Fluorescence ratio imaging of cyclic AMP in single cells. *Nature*. 349:694–697.
- Augustine, G.J., F. Santamaria, and K. Tanaka. 2003. Local calcium signaling in neurons. *Neuron*. 40:331–346.
- Averill, S., S.B. McMahon, D.O. Clary, L.F. Reichardt, and J.V. Priestley. 1995. Immunocytochemical localization of trkA receptors in chemically identified subgroups of adult rat sensory neurons. *Eur. J. Neurosci*. 7:1484–1494.
- Bouchard, R., R. Pattarini, and J.D. Geiger. 2003. Presence and functional significance of presynaptic ryanodine receptors. *Prog. Neurobiol.* 69:391–418.
- Brummendorf, T., and F.G. Rathjen. 1994. Cell adhesion molecules. 1: immunoglobulin superfamily. *Protein Profile*. 1:951–1058.
- Cai, D., Y. Shen, M. De Bellard, S. Tang, and M.T. Filbin. 1999. Prior exposure to neurotrophins blocks inhibition of axonal regeneration by MAG and myelin via a cAMP-dependent mechanism. *Neuron*. 22:89–101.
- Castellani, V., A. Chedotal, M. Schachner, C. Faivre-Sarrailh, and G. Rougon. 2000. Analysis of the L1-deficient mouse phenotype reveals cross-talk between Sema3A and L1 signaling pathways in axonal guidance. *Neuron*. 27:237–249.
- Castellani, V., E. De Angelis, S. Kenwrick, and G. Rougon. 2002. Cis and trans interactions of L1 with neuropilin-1 control axonal responses to semaphorin 3A. *EMBO J*. 21:6348–6357.
- Cheng, S., M.S. Geddis, and V. Rehder. 2002. Local calcium changes regulate the length of growth cone filopodia. *J. Neurobiol.* 50:263–275.
- Davenport, R.W., P. Dou, V. Rehder, and S.B. Kater. 1993. A sensory role for neuronal growth cone filopodia. *Nature*. 361:721–724.
- Doherty, P., G. Williams, and E.J. Williams. 2000. CAMs and axonal growth: a critical evaluation of the role of calcium and the MAPK cascade. *Mol. Cell. Neurosci*. 16:283–295.
- Futatsugi, A., K. Kato, H. Ogura, S.T. Li, E. Nagata, G. Kuwajima, K. Tanaka, S. Itohara, and K. Mikoshiba. 1999. Facilitation of NMDAR-independent LTP and spatial learning in mutant mice lacking ryanodine receptor type 3. *Neuron*. 24:701–713.
- Gibson, S.J., J.M. Polak, S.R. Bloom, I.M. Sabate, P.M. Mulderry, M.A. Ghatei, G.P. McGregor, J.F. Morrison, J.S. Kelly, and R.M. Evans. 1984. Calcitonin gene-related peptide immunoreactivity in the spinal cord of man and of eight other species. *J. Neurosci*. 4:3101–3111.
- Gomez, T.M., and N.C. Spitzer. 1999. In vivo regulation of axon extension and pathfinding by growth-cone calcium transients. *Nature*. 397:350–355.
- Gomez, T.M., E. Robles, M. Poo, and N.C. Spitzer. 2001. Filopodial calcium transients promote substrate-dependent growth cone turning. *Science*. 291:1983–1987.
- Grynkiewicz, G., M. Poenie, and R.Y. Tsien. 1985. A new generation of Ca²⁺ indicators with greatly improved fluorescence properties. *J. Biol. Chem.* 260:3440–3450.
- Henley, J.R., K.H. Huang, D. Wang, and M.M. Poo. 2004. Calcium mediates bidirectional growth cone turning induced by myelin-associated glycoprotein. *Neuron*. 44:909–916.
- Hong, K., M. Nishiyama, J. Henley, M. Tessier-Lavigne, and M. Poo. 2000. Calcium signalling in the guidance of nerve growth by netrin-1. *Nature*. 403:93–98.
- Hopker, V.H., D. Shewan, M. Tessier-Lavigne, M. Poo, and C. Holt. 1999. Growth-cone attraction to netrin-1 is converted to repulsion by laminin-1. *Nature*. 401:69–73.
- Huber, A.B., A.L. Kolodkin, D.D. Ginty, and J.F. Cloutier. 2003. Signaling at the growth cone: ligand-receptor complexes and the control of axon growth and guidance. *Annu. Rev. Neurosci.* 26:509–563.
- Kamiguchi, H., and F. Yoshihara. 2001. The role of endocytic L1 trafficking in polarized adhesion and migration of nerve growth cones. *J. Neurosci*. 21:9194–9203.
- Kuhn, T.B., C.V. Williams, P. Dou, and S.B. Kater. 1998. Laminin directs growth cone navigation via two temporally and functionally distinct calcium signals. *J. Neurosci*. 18:184–194.
- Kuwajima, G., A. Futatsugi, M. Niinobe, S. Nakanishi, and K. Mikoshiba. 1992. Two types of ryanodine receptors in mouse brain: skeletal muscle type exclusively in Purkinje cells and cardiac muscle type in various neurons. *Neuron*. 9:1133–1142.
- Lau, P.M., R.S. Zucker, and D. Bentley. 1999. Induction of filopodia by direct local elevation of intracellular calcium ion concentration. *J. Cell Biol.* 145:1265–1275.
- Letourneau, P.C., M.L. Condic, and D.M. Snow. 1994. Interactions of developing neurons with the extracellular matrix. *J. Neurosci*. 14:915–928.
- Lev-Ram, V., H. Miyakawa, N. Lasser-Ross, and W.N. Ross. 1992. Calcium transients in cerebellar Purkinje neurons evoked by intracellular stimulation. *J. Neurophysiol.* 68:1167–1177.
- Lokuta, A.J., H. Komai, T.S. McDowell, and H.H. Valdivia. 2002. Functional properties of ryanodine receptors from rat dorsal root ganglia. *FEBS Lett.* 511:90–96.
- Nakai, Y., and H. Kamiguchi. 2002. Migration of nerve growth cones requires detergent-resistant membranes in a spatially defined and substrate-dependent manner. *J. Cell Biol.* 159:1097–1108.
- Neumann, S., F. Bradke, M. Tessier-Lavigne, and A.I. Basbaum. 2002. Regeneration of sensory axons within the injured spinal cord induced by intraganglionic cAMP elevation. *Neuron*. 34:885–893.
- Nishimura, K., F. Yoshihara, T. Tojima, N. Ooashi, W. Yoon, K. Mikoshiba, V. Bennett, and H. Kamiguchi. 2003. L1-dependent neuriteogenesis involves ankyrin_β that mediates L1-CAM coupling with retrograde actin flow. *J. Cell Biol.* 163:1077–1088.
- Nishiyama, M., A. Hoshino, L. Tsai, J.R. Henley, Y. Goshima, M. Tessier-Lavigne, M.M. Poo, and K. Hong. 2003. Cyclic AMP/GMP-dependent modulation of Ca²⁺ channels sets the polarity of nerve growth-cone turning. *Nature*. 423:990–995.
- Perrin, F.E., F.G. Rathjen, and E.T. Stoeckli. 2001. Distinct subpopulations of sensory afferents require F11 or axonin-1 for growth to their target layers within the spinal cord of the chick. *Neuron*. 30:707–723.
- Qiu, J., D. Cai, H. Dai, M. McAttee, P.N. Hoffman, B.S. Bregman, and M.T. Filbin. 2002. Spinal axon regeneration induced by elevation of cyclic AMP. *Neuron*. 34:895–903.
- Robles, E., A. Huttenlocher, and T.M. Gomez. 2003. Filopodial calcium transients regulate growth cone motility and guidance through local activation of calpain. *Neuron*. 38:597–609.
- Snider, W.D. 1994. Functions of the neurotrophins during nervous system development: what the knockouts are teaching us. *Cell*. 77:627–638.
- Song, H.J., and M.M. Poo. 1999. Signal transduction underlying growth cone guidance by diffusible factors. *Curr. Opin. Neurobiol.* 9:355–363.
- Sydney, A.M., A.L. Su, F.S. Wang, A. Xu, and D.G. Jay. 1996. Talin and vinculin play distinct roles in filopodial motility in the neuronal growth cone. *J. Cell Biol.* 134:1197–1207.
- Takei, K., R.M. Shin, T. Inoue, K. Kato, and K. Mikoshiba. 1998. Regulation of nerve growth mediated by inositol 1,4,5-trisphosphate receptors in growth cones. *Science*. 282:1705–1708.
- Takeichi, M. 1991. Cadherin cell adhesion receptors as a morphogenetic regulator. *Science*. 251:1451–1455.
- Tang, F., E.W. Dent, and K. Kalil. 2003. Spontaneous calcium transients in developing cortical neurons regulate axon outgrowth. *J. Neurosci*. 23:927–936.
- Tessier-Lavigne, M., and C.S. Goodman. 1996. The molecular biology of axon guidance. *Science*. 274:1123–1133.
- Valdivia, H.H., J.H. Kaplan, G.C. Ellis-Davies, and W.J. Lederer. 1995. Rapid adaptation of cardiac ryanodine receptors: modulation by Mg²⁺ and phosphorylation. *Science*. 267:1997–2000.
- Wehrens, X.H., and A.R. Marks. 2003. Altered function and regulation of cardiac ryanodine receptors in cardiac disease. *Trends Biochem. Sci.* 28:671–678.
- Wen, Z., C. Guirland, G.L. Ming, and J.Q. Zheng. 2004. A CaMKII/calcineurin switch controls the direction of Ca²⁺-dependent growth cone guidance. *Neuron*. 43:835–846.
- Yoshida, A., A. Ogura, T. Imagawa, M. Shigekawa, and M. Takahashi. 1992. Cyclic AMP-dependent phosphorylation of the rat brain ryanodine receptor. *J. Neurosci*. 12:1094–1100.
- Zheng, J.Q. 2000. Turning of nerve growth cones induced by localized increases in intracellular calcium ions. *Nature*. 403:89–93.
- Zucchi, R., and S. Ronca-Testoni. 1997. The sarcoplasmic reticulum Ca²⁺ channel/ryanodine receptor: modulation by endogenous effectors, drugs and disease states. *Pharmacol. Rev.* 49:1–51.